Available online at www.sciencedirect.com
SCIENCE DIRECT®
Polyhedron 24 (2005) 2505–2512
POLYHEDRON
www.elsevier.com/locate/poly

Two isomeric $[Mn_{12}O_{12}(OMe)_2(O_2CPh)_{16}(H_2O)_2]^{2-}$ single-molecule magnets and a Mn^{III} polymer prepared by a reductive aggregation synthetic route

Anastasios J. Tasiopoulos [a,1], Wolfgang Wernsdorfer [b], Khalil A. Abboud [a], George Christou [a,*]

[a] Department of Chemistry, University of Florida, Gainesville, FL 32611-7200, USA
[b] Laboratoire Louis Néel-CNRS, BP 166, 25 Avenue des Martyrs, 38042 Grenoble, Cedex 9, France

Received 5 October 2004; accepted 5 December 2004
Available online 17 May 2005

Abstract

We describe a new synthetic procedure in Mn cluster chemistry involving reductive aggregation of permanganate (MnO_4^-) ions in MeOH/benzoic acid solution and the first two products that were obtained from this procedure. The first one is the anion $[Mn_{12}O_{12}(OMe)_2(O_2CPh)_{16}(H_2O)_2]^{2-}$ which was isolated as a black microcrystalline material when the solution was left at room temperature overnight. The microcrystalline material was recrystallized from CH_2Cl_2/hexanes and gave the above mentioned anion as a mixture of two crystal forms $(N^nBu_4)_2[Mn_{12}O_{12}(OMe)_2(O_2CPh)_{16}(H_2O)_2]\cdot 2H_2O\cdot 4CH_2Cl_2$ and $(N^nBu_4)_2[Mn_{12}O_{12}(OMe)_2(O_2CPh)_{16}(H_2O)_2]\cdot 2H_2O\cdot CH_2Cl_2$. The anion contains a central $[Mn^{IV}_4(\mu_3\text{-}O)_2(\mu\text{-}O)_2(\mu\text{-}OMe)_2]^{6+}$ unit surrounded by a non-planar ring of eight Mn^{III} atoms that are connected to the central Mn_4 unit by eight bridging $\mu_3\text{-}O^{2-}$ ions. This anion is remarkably similar to the well known $[Mn_{12}O_{12}(O_2CR)_{16}(H_2O)_4]$ complexes (hereafter called "normal $[Mn_{12}]$"), with the main difference being the structure of the central cores. The second compound was the polymeric $[Mn(OMe)(O_2CPh)_2]_n$ that was obtained when the solution was left at room temperature for ~2 weeks. The compound contains a linear chain of repeating $[Mn^{III}(\mu\text{-}O_2CPh)_2(\mu\text{-}OMe)Mn^{III}]$ units. The chains are parallel to each other and are interacting weakly through π-stacking between the benzoate rings of different chains. Variable temperature ac magnetic measurements and hysteresis studies revealed that both anions are SMMs and like normal $[Mn_{12}]$ clusters, display both faster- and slower-relaxing magnetization dynamics that we assign to the presence of JT isomerism. Variable temperature magnetic susceptibility studies establish that the Mn^{III} centers of the polymer are antiferromagnetically coupled resulting in a diamagnetic ground state.

Keywords: Reductive aggregation; Permanganate; Single-molecule magnet; Magnetic properties

1. Introduction

An exciting development in nanoscale magnetic materials occurred in 1993 when $[Mn_{12}O_{12}(O_2CMe)_{16}(H_2O)_4]$ (**1**) was identified as a nanoscale magnet [1], the first to comprise discrete (magnetically), non-interacting molecular units rather than a 3D extended lattice (metals, metal oxides, etc). This discovery initiated the field of molecular nanomagnetism and such molecules have since been termed single-molecule magnets (SMMs) [2]. They derive their properties from the combination of a large spin (S) and an Ising (easy-axis) magnetoanisotropy (negative zero-field splitting parameter, D). Although several classes of SMMs are now

* Corresponding author. Tel.: +1 352 392 8314; fax: +1 352 392 8757.
E-mail addresses: atasio@ucy.ac.cy (A.J. Tasiopoulos), christou@chem.ufl.edu (G. Christou).
[1] Present address: Department of Chemistry, University of Cyprus, 1678 Nicosia, Cyprus. Tel.: +35722892765; fax: +35722892801.

0277-5387/$ - see front matter © 2005 Elsevier Ltd. All rights reserved.
doi:10.1016/j.poly.2005.03.074

known [1–10], there is a continuing need for new examples to improve our understanding of this phenomenon. Efforts along these lines have been concentrated in two directions: (i) development of synthetic routes to new high nuclearity metal complexes [4,5], and (ii) modifications of known SMMs in a controlled fashion [6–10]. The best and most thoroughly studied SMMs to date are members of the $[Mn_{12}O_{12}(O_2CR)_{16}(H_2O)_4]$ ($[Mn_{12}]$) family. A number of $[Mn_{12}]$ derivatives have been prepared in their neutral [1,6–8], one-electron [6f,9] or two-electron [10] reduced versions with a variety of carboxylate [6,9,10], mixed carboxylate [7], and mixed carboxylate/non-carboxylate [8] ligands. In all such modifications, the $[Mn_{12}(\mu_3\text{-}O)_{12}]$ core remains essentially the same.

In the present work, we report three new developments: (i) A new synthetic procedure in Mn cluster chemistry involving reductive aggregation of permanganate (MnO_4^-) ions in MeOH/benzoic acid solution; (ii) the products of this synthetic procedure which include two new compounds, the $N^nBu_4^+$ salts of the new $[Mn_{12}O_{12}(OMe)_2(O_2CPh)_{16}(H_2O)_2]^{2-}$ (**2**) cluster anion, a structural derivative of the well studied $[Mn_{12}]$ complexes, and the polymer $[Mn(OMe)(O_2CPh)_2]_n$ (**3**); and (iii) the establishment that the anion of **2** is a new SMM.

2. Experimental

2.1. Syntheses

All manipulations were performed under aerobic conditions with the use of materials as received unless otherwise indicated; water was distilled in-house. Elemental analyses were performed by the in-house facilities of the Chemistry Department, University of Florida.

2.1.1. Preparation of $(N^nBu_4)_2[Mn_{12}O_{12}(O_2CPh)_{16}(OMe)_2(H_2O)_2]$ (2)

Freshly prepared $(N^nBu_4)MnO_4$ (1.0 g, 2.8 mmol) was added in small portions to a solution of benzoic acid (5.0 g, 40.9 mmol) in MeOH (15 ml), and the mixture stirred for ~5 min. The resulting purple solution was left undisturbed at room temperature overnight. During this time, the color slowly turned dark brown, and black crystals slowly formed. The latter, which were found to be poor diffractors of X-rays, were collected by filtration, washed with MeOH (2 × 10 ml) and dried in vacuo. The material was recrystallized from CH_2Cl_2/hexanes to give a mixture of diamond-shaped crystals of $2 \cdot 2H_2O \cdot 4CH_2Cl_2$ (**2a**) and needle-shaped crystals of $2 \cdot 2H_2O \cdot CH_2Cl_2$ (**2b**) in an overall yield of 0.12 g (15 % based on Mn). These were collected by filtration, washed with hexanes, and dried in vacuo. Both **2a** and **2b** were good diffractors of X-rays, as long as they were kept in contact with the mother liquor to prevent solvent loss. *Anal.* Calc. for $C_{146}H_{166}N_2O_{50}Mn_{12}$ ($2 \cdot 2H_2O$): C, 51.45; H, 4.91; N, 0.82. Found: C, 51.26; H, 4.72; N, 0.70%. Selected IR data (KBr, cm^{-1}): 3430(s, br), 3065(w) 2965(w), 2925(w), 2875(w), 1598(s), 1560(s), 1532(s), 1492(m), 1448(m), 1417(s), 1306(w), 1177(m), 1069(w), 1026(m), 838(w), 718(s), 675(s), 625(m, br), 499(m).

2.1.2. Preparation of $[Mn(OMe)(O_2CPh)_2]_n$ (3)

Compound **3** was prepared by employing the same synthetic procedure as for **2** with the only difference being that the purple solution was left to stand at room temperature for a long period of time (~2 weeks). The yield was 70%. *Anal.* Calc. for $C_{15}H_{13}MnO_5$ (**3**): C, 54.90; H: 3.99. Found: C, 54.67; H, 3.83%. Selected IR data (KBr, cm^{-1}): 3421(m, br), 3065(m), 3023(w), 2940(w), 1693(m), 1592(s), 1552(s), 1491(m), 1448(m), 1386(s), 1306(m), 1177(m), 1159(w), 1143(w), 1069(m), 1026(m), 992(m), 937(w), 841(w), 816(w), 716(s), 683(m), 610(m), 558(m), 483(m).

3. Results and discussion

3.1. Syntheses

The synthesis of normal $[Mn_{12}]$ compound **1** consists of the comproportionation reaction between $Mn(O_2CMe)_2 \cdot 4H_2O$ and $KMnO_4$ in 60% aqueous acetic acid [11]. In contrast, the new synthetic procedure in the present work is part of a wider investigation of the reduction of MnO_4^- in alcohol/carboxylic acid mixtures. The present results were obtained from a MeOH/$PhCO_2H$ medium. Thus, addition of $(N^nBu_4)MnO_4$ to a methanolic solution of benzoic acid results in the formation of a dark brown solution from which subsequently were obtained essentially black crystals. Recrystallization from CH_2Cl_2/hexanes results in the formation of two types of black crystals in a total, overall yield of 15% yield. When the dark brown solution was left for ~2 weeks to stand at room temperature brown crystals of **3** were formed in high yield. Since the average oxidation state of **2** (8 Mn^{III}, 4 Mn^{IV}) is higher than that of **3** (Mn^{III}), it seems reasonable to assume that the formation of the latter is a result of further reduction of Mn^{IV} ions by MeOH, i.e., the longer crystallization times allow the formation of products that are further reduced.

3.2. Description of structures

3.2.1. $[Mn_{12}O_{12}(OMe)_2(O_2CPh)_{16}(H_2O)_2]^{2-}$

Both types of crystals of **2**, diamond-like **2a** and needle-like **2b**, were crystallographically characterized, and found to be $(N^nBu_4)_2[Mn_{12}O_{12}(OMe)_2(O_2CPh)_{16}(H_2O)_2] \cdot 2H_2O \cdot 4CH_2Cl_2$ (**2a**) and $(N^nBu_4)_2[Mn_{12}O_{12}$-

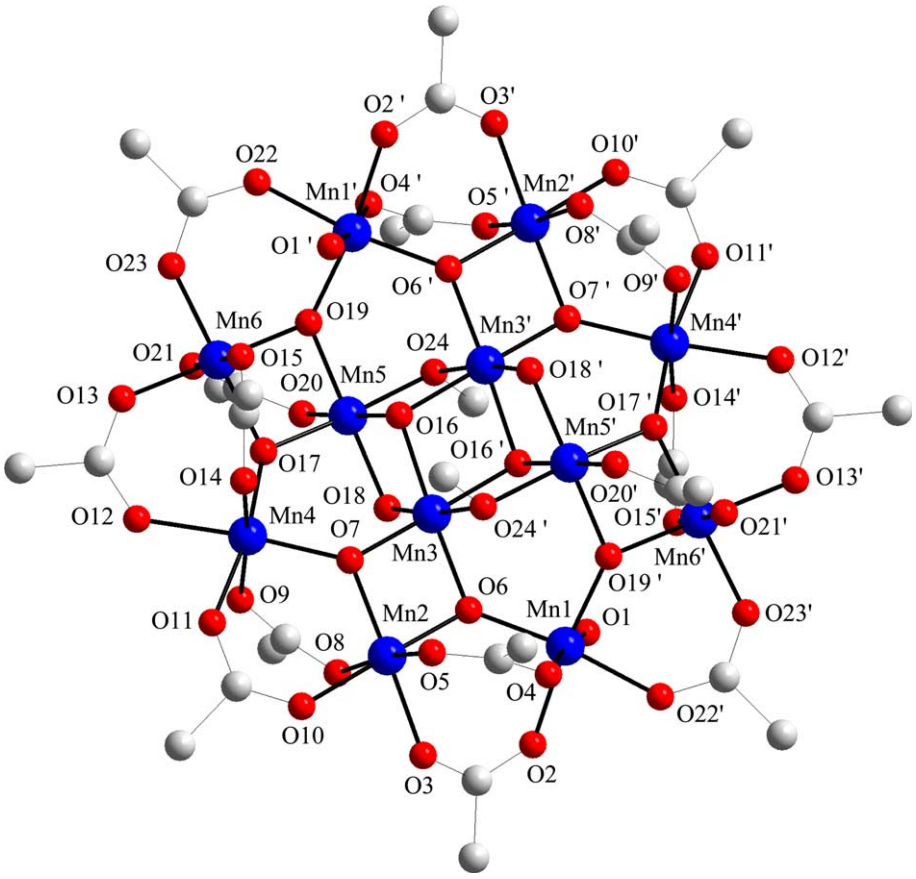

Fig. 1. Labeled ORTEP plot (at the 50% probability level) of the anion of **2a**. For clarity, the benzoate rings have been omitted, except for the *ipso*-carbon atom of each ring. Color scheme: Mn (blue), O (red), C (grey).

$(OMe)_2(O_2CPh)_{16}(H_2O)_2]\cdot 2H_2O\cdot CH_2Cl_2$ (**2b**). Both contain the same dianion, abbreviated $[Mn_{12}']^{2-}$. Complex **2a** crystallizes in the orthorhombic space group *Pbca* with its asymmetric unit containing half the $[Mn_{12}']^{2-}$ cluster and one $N^nBu_4^+$ cation, as well as one H_2O and two disordered CH_2Cl_2 solvent molecules. The $[Mn_{12}']^{2-}$ anion of **2a** (Fig. 1) contains a central $[Mn^{IV}_4(\mu_3\text{-}O)_2(\mu\text{-}O)_2(\mu\text{-}OMe)_2]^{6+}$ unit surrounded by a non-planar ring of eight Mn^{III} atoms that are connected to the central Mn_4 unit by eight bridging $\mu_3\text{-}O^{2-}$ ions. The metal oxidation states and their trapped-valence nature were determined by inspection of the Mn–O bond lengths, Mn bond valence sum calculations[2] [12] and the presence of Mn^{III} Jahn–Teller elongation axes for the Mn atoms in the outer ring. The outer Mn_8 ring is very similar to that in normal $[Mn_{12}]$ compound **1**, but the latter has a central $[Mn_4(\mu_3\text{-}O)_4]^{8+}$ cubane. The central $[Mn^{IV}_4O_4(OMe)_2]^{6+}$ unit of **2a** comprises a planar Mn_4 rhombus with two $\mu_3\text{-}O^{2-}$ ions (O16, O16′), one above and one below the Mn_4 plane, and a $\mu\text{-}O^{2-}$ (O18, O18′) or $\mu\text{-}MeO^-$ (O24, O24′) ion bridging each edge of the rhombus. The central unit can thus be described either as a face-sharing dicubane unit with two missing vertices, or as two edge-sharing, oxide-capped Mn_3 triangular units. Tetranuclear complexes possessing a core very similar to this central unit of the anion of **2a** have been observed previously with Mn [5a,5b], as well as with other transition metals [13]. Peripheral ligation is completed by 16 bridging benzoate groups and two terminal water molecules. All Mn atoms are six-coordinate with near octahedral geometries.

Complex **2b** crystallizes in the triclinic space group $P\bar{1}$, and its asymmetric unit consists of a half cluster and two halves of $N^nBu_4^+$ cations disordered around inversion centers, as well as one disordered H_2O molecule and half a CH_2Cl_2. The structure of the anion of **2b** is essentially identical to that of **2a**, except for some disorder in the peripheral benzoate rings.

For both **2a** and **2b**, there are Jahn–Teller (JT) distortions at the Mn^{III} ions in the outer ring, consistent with high-spin Mn^{III} in near-octahedral geometry. The JT distortion takes the form of an axial elongation, with the elongation axes axial to the Mn_{12} disk-like core and thus roughly parallel to each other. Axially elon-

[2] Bond valence sum calculations for Mn^{III} and Mn^{IV} ions of **2a** and **2b** gave oxidation state values of 2.89–3.02 and 4.00–4.18, respectively.

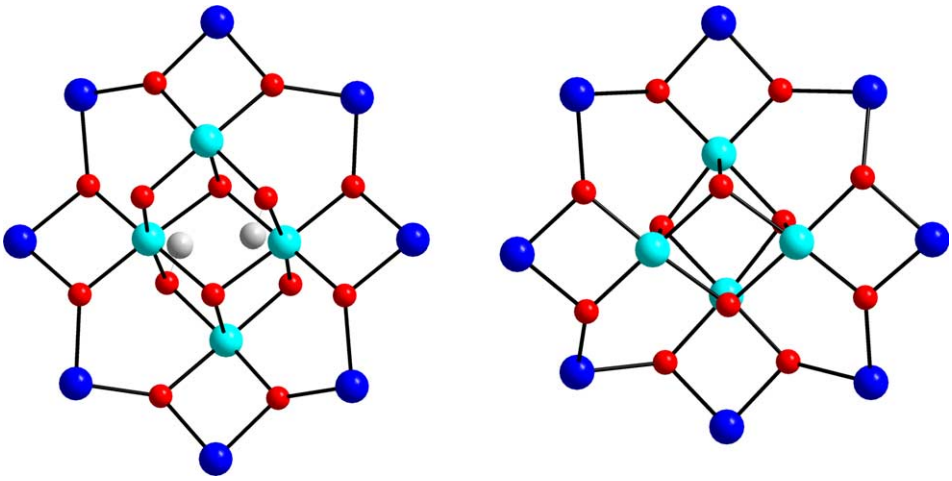

Fig. 2. Comparison of the cores of the anion of **2a** (left) and normal [Mn_{12}] complex **1** (right). Color scheme: Mn^{4+} (cyan), Mn^{3+} (blue), O (red), C (grey).

gated Mn–O bonds are typically at least 0.1–0.2 Å longer than the others. However, there is one anomaly: for **2a** (Fig. 1), the JT elongated bonds at Mn4 (Mn4–O9 = 2.074(4), Mn4–O14 = 2.080(5) Å) are not as long as those at the other Mn^{III} ions (2.112(5)–2.250(5) Å), and *trans* bonds Mn4–O7 (1.958(4) Å) and Mn4–O12 (2.060(5) Å) are longer than expected, especially Mn–O7, which is unusually long for a Mn–O^{2-} bond (compare Mn–O^{2-} bonds at the other Mn^{III} ions of 1.876(4)–1.905(4) Å). A similar anomalous situation is present at Mn1 of **2b**. This structural feature at Mn atoms Mn4 of **2a** and Mn1 of **2b** will prove crucial to understanding the magnetic data below, and we will thus return to this point later.

The anions of complexes **2a** and **2b** are remarkably similar to normal [Mn_{12}] clusters, such as **1**, with the main difference being the structure of the central cores. These are compared in Fig. 2. In fact, the core of the anions of **2a** and **2b** could be considered the result of partial methanolysis of the central $[Mn_4O_4]^{8+}$ cubane of **1**, leading to incorporation of two MeO^- bridges and a change in the core structure (although we do not claim that this corresponds to its means of formation in the reaction mixture). It is also interesting to note that complexes **1** and **2** are the smallest nuclearity members of a larger family of [Mn^{III}_x, Mn^{IV}_y] clusters in which there is an outer Mn^{III}_x ring around a central Mn^{IV}_y core. This family currently comprises normal [Mn_{12}] complexes (such as **1**) and **2a/2b** ($x = 8, y = 4$), the Mn_{16} cluster $[Mn_{16}O_{16}(OMe)_6(O_2CMe)_{16}(MeOH)_3(H_2O)_3]$ ($x = 10$, $y = 6$) [4c,14], and the Mn_{21} cluster $[Mn_{21}O_{24}(OMe)_8(O_2CCH_2{}^tBu)_{16}(H_2O)_{10}]$ ($x = 12, y = 9$) [15].

3.2.2. $[Mn(OMe)(O_2CPh)_2]_n$

Compound **3** crystallizes in the triclinic space group $P\bar{1}$ and its asymmetric unit consists of a [Mn(μ-O_2CPh)$_2$(μ-OMe)Mn] portion of the chain. The compound contains a linear chain of repeating [Mn^{III}(μ-OMe)(μ-O_2CPh)$_2$$Mn^{III}$] units (Fig. 3). The structure of **3** is similar to that of {[Mn(OH)(O_2CMe)$_2$] · HO_2CMe · H_2O} (**4**) reported recently [16], which is also a linear chain, except that (i) there are OMe^- bridging groups instead of OH^-, (ii) the carboxylate ligands are $PhCO_2^-$ instead of $MeCO_2^-$, and (iii) there are no solvents of crystallization in contrast to **4** where solvents of crystallization are participating in the formation of a hydrogen-bonding network between chains. The Mn···Mn separations in **3** are 3.388(1) Å, identical to the 3.384(1) Å value of those in **4**. All the $PhCO_2^-$ groups are in their familiar *syn*,*syn*-bridging modes. The metal oxidation state and its trapped-valence nature were determined by inspection of the Mn–O bond

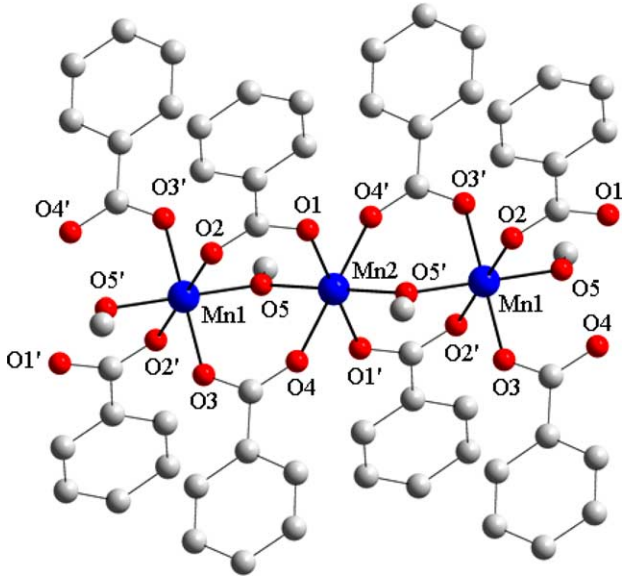

Fig. 3. Labelled ORTEP plot (at the 50% probability level) of a small section of the polymeric chain of [Mn(OMe)(O_2CPh)$_2$]$_n$ (**3**).

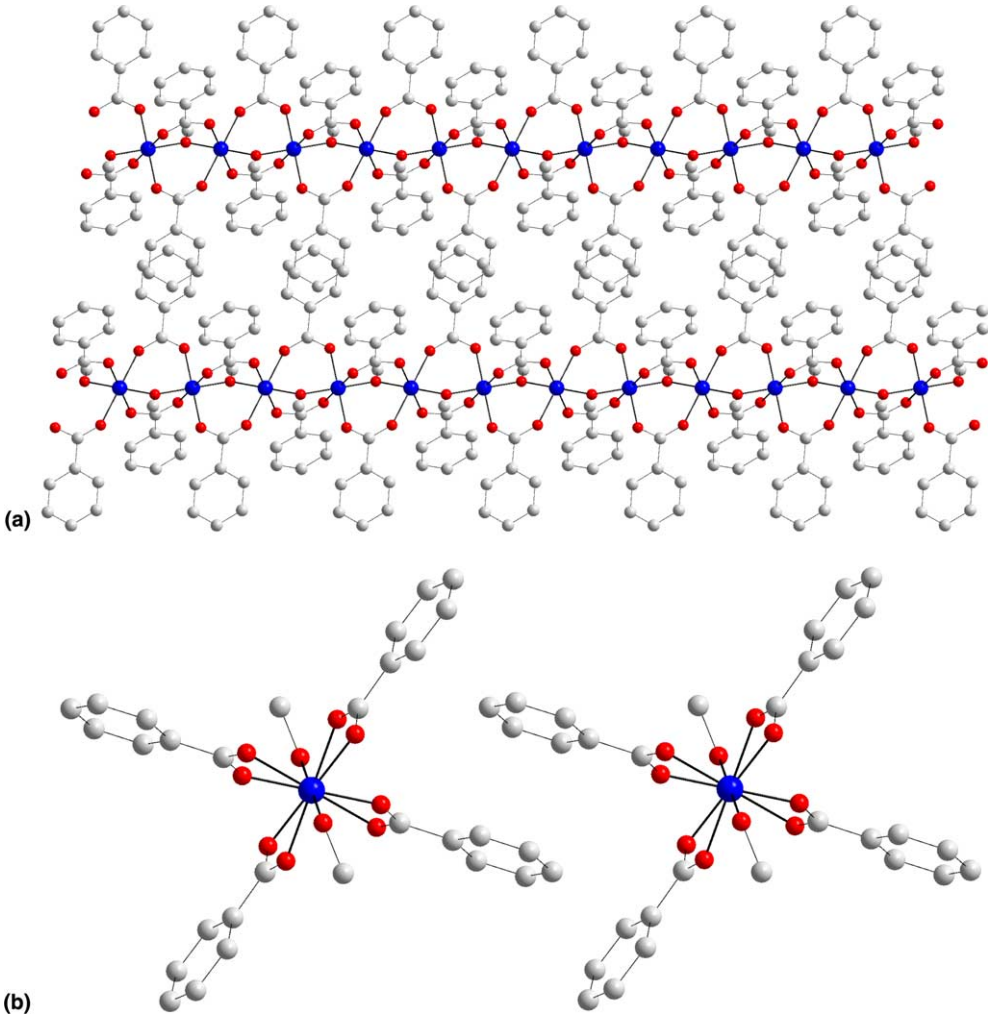

Fig. 4. (a) A section of two adjacent chains of **3** emphasizing (i) the π-stacking between the benzoate rings of the two neighboring chains, (ii) the fact that the chains run parallel in the crystal. (b) A view along the chain axis of **1**.

lengths, Mn bond valence sum calculations[3] [12] and the presence of Mn^{III} Jahn–Teller elongation axes for the two independent Mn atoms of the chain. The Jahn–Teller elongation axes are the O(2)–Mn(1)–O(2′) and O(4′)–Mn–O(2), which are parallel. It is interesting to note that the [Mn(μ-OMe)(μ-$O_2CR)_2$Mn] triply bridged unit is unprecedented in any Mn cluster of any nuclearity. This could be partially due to the fact that the list of Mn complexes containing methoxy groups is not extensive. A close examination of the packing of **3** shows that the chains all run parallel in the crystal, and in the absence of solvent molecules of crystallization there are no hydrogen-bonding interactions holding the neighboring chains together. However, a closer look reveals the existence of π-stacking interactions between the benzoate rings of neighboring chains (average C···C separation = 3.719 Å). This is emphasized in Fig. 4, which shows a small part of two adjacent chains from a viewpoint perpendicular to the chains (Fig. 4(a)) and along the chains (Fig. 4(b)).

3.3. Magnetism studies

3.3.1. $[Mn_{12}O_{12}(OMe)_2(O_2CPh)_{16}(H_2O)_2]^{2-}$

The structural similarity between complexes **1** and **2** suggested the possibility that the latter might also be a SMM, just like the former. This was therefore investigated by AC magnetic susceptibility measurements on a polycrystalline sample of **2** (containing both **2a** and **2b**) in the temperature range 1.8–10 K using a 3.5 G AC field oscillating at 5–500 Hz frequencies (ν). These studies revealed two frequency-dependent out-of-phase χ''_m AC signals (Fig. 5), one in the higher temperature (HT) range of 3–5 K, and a second one at lower temperatures (LT) whose peaks clearly occur at temperatures below the operating limit of our SQUID (superconducting quantum interference device) instrument (1.8 K).

[3] Bond valence sum calculations for the two independent Mn^{III} ions of **3** gave oxidation state values of 2.98 for both of them.

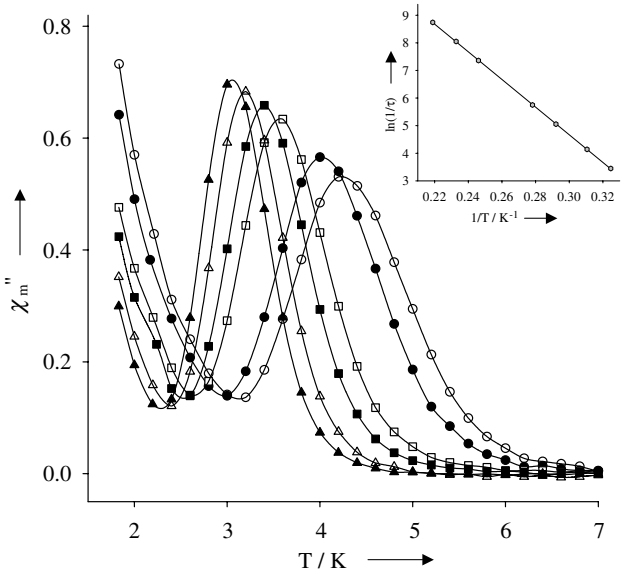

Fig. 5. Plot of χ''_m vs. T for a microcrystalline sample of **2** at 500 (○), 250 (●), 50 (□), 25 (■), 10 (△), 5 (▲) Hz. Inset: Plot of the natural logarithm of relaxation rate, $\ln(1/\tau)$ vs. inverse temperature using the χ''_m vs. T data for the slower-relaxing species (higher temperature data). The solid line is a fit to the Arrhenius equation; see the text for the fitting parameters.

The LT and HT χ''_m signals correspond to faster and slower relaxation rates, respectively. The peak of a χ''_m versus T plot represents the temperature at which the magnetization relaxation rate equals the angular frequency $\omega(=2\pi\nu)$, and the χ''_m versus T data at different frequencies (ν) were therefore used as a source of kinetic data to construct an Arrhenius plot (Fig. 5, inset) based on the Arrhenius equation of Eq. (1), where $1/\tau$ is the relaxation rate (τ is the relaxation time), $1/\tau_0$ is the pre-exponential factor, U_{eff} is the effective relaxation barrier,

$$1/\tau = 1/\tau_0 \exp(-U_{eff}/kT) \quad (1)$$

and k is the Boltzmann constant. The fit of the data to Eq. (1) gave $U_{eff} = 50.1$ K and $1/\tau_0 = 3.61 \times 10^8$ s^{-1}. This U_{eff} value is smaller than that of normal [Mn_{12}] complexes; complex **1**, for example, has a U_{eff} of 60–65 K.

The observation of out-of-phase AC signals suggests that **2** might be an SMM, although such signals by themselves are not proof of an SMM. It is also tempting to assume that the two χ''_m signals in Fig. 3 are due to the two crystal forms, diamond-like **2a** and needle-like **2b**. To confirm whether **2a** and/or **2b** are indeed SMMs, and to assess any difference between the two forms, magnetization versus DC field sweep studies were performed on single crystals of **2a** and **2b** using a micro-SQUID apparatus [17]. The resulting hysteresis loops are shown in Fig. 6, and their coercivities (i) increase with decreasing T at a constant field sweep rate, and (ii) increase with increasing sweep rate at a constant T

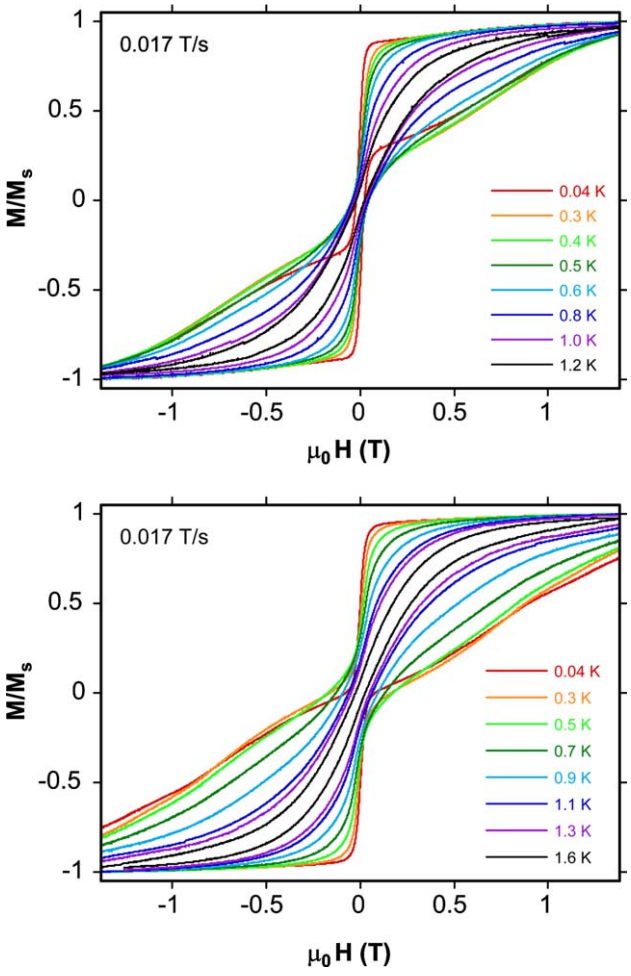

Fig. 6. Magnetization (M) vs. applied magnetic field ($\mu_0 H$) hysteresis loops for a single crystal (wet with mother liquor) of **2a** (top) and **2b** (bottom) at the indicated temperatures. M is normalized to its saturation value, M_s.

(not shown). This is as expected for the superparamagnet-like properties of a SMM.

However, it is clear that the observed properties (hysteresis loops) of **2a** and **2b** are very similar, and this is totally inconsistent with the two very different AC signals in Fig. 5 and the at-first-glance 'obvious' conclusion that the two signals are due to the two crystal forms. In fact, the hysteresis loops of both **2a** and **2b** each suggest a mixture of faster-relaxing (LT) and slower-relaxing (HT) forms, the former being responsible for the large decrease in magnetization at zero field, and the latter being responsible for the subsequent feature at higher fields. The relative proportions of these two features suggest comparable amounts of the LT and HT forms in each crystal, with perhaps a slightly greater amount of the former, and this is again consistent with the relative proportion of LT and HT AC signals in Fig. 5. Note that the AC and hysteresis studies were performed on wet single-crystals and microcrystals suspended in solid eicosane, respectively, and thus not strictly speaking on

the same material. Nevertheless, we conclude that (i) complex **2** is a new SMM; (ii) the different space groups of diamond-like **2a** and needle-like **2b** lead to only small differences in the magnetic properties of the $[Mn_{12}O_{12}(OMe)_2(O_2CPh)_{16}(H_2O)_2]^{2-}$ anion; and (iii) there are faster- and slower-relaxing forms of complex **2** that co-crystallize in the same crystal. In fact, point (iii) has long been known to also be the case for **1**, whose crystals contain about 5% of the faster-relaxing form; complex **2** thus differs from **1** only in the relative amounts of the two forms.

For normal $[Mn_{12}]$ complexes, we have reported elsewhere that crystals of pure faster-relaxing forms can be prepared with, for example, ^{t}butylacetate as the carboxylate group [6d,6g]. Crystallography on such crystals has allowed the origin of the faster-relaxing form to be identified as the abnormal orientation of one of the Mn^{III} JT elongation axes being disposed equatorial rather than axial to the Mn_{12} disk-like plane, and thus pointing to a core O^{2-} ion. We have named this 'Jahn–Teller isomerism'. The same is likely to be the origin of the two forms of **2**. Indeed, this takes us back full circle to the crystal structures described above, because it rationalizes the unusual Mn–O bond lengths at Mn4 for **2a** and Mn1 for **2b**. For **2a**, for example, an approximately equal mixture of (a) slower-relaxing species with the JT axis at Mn4 in the normal position along the O9–Mn4–O14 axis, and (b) faster-relaxing species with the JT axis at Mn4 abnormally aligned along the O7–Mn4–O12 axis will lead to the crystallographic average result that the O9–Mn4–O14 and O7–Mn4–O12 bond lengths are shorter and longer, respectively, than they should be, which is what is seen. Similarly for **2b**, we thus feel that the crystallographic data support the conclusion from the magnetic studies that crystals of **2a** and **2b** comprise a mixture of slower- and faster-relaxing species resulting from normal and abnormal orientations, respectively, of a Mn^{III} JT elongation axis. As with normal $[Mn_{12}]$ complexes, it will require crystallization of pure crystals of the different forms of **2** to allow more detailed study, and this is a current objective.

3.3.2. $[Mn(OMe)(O_2CPh)_2]_n$

Solid state dc magnetic susceptibility data were collected in the 5.0–300 K range in a 5 kG (0.5 T) field. The data for **3** are plotted as $\chi_m T$ versus T in Fig. 7. The $\chi_m T$ value of 2.59 $cm^3\ mol^{-1}$ K at 300 K is lower than the expected value of 3 $cm^3\ mol^{-1}$ K for an isolated Mn^{III} center, and decreases steadily to 0.18 $cm^3\ mol^{-1}$ K at 8 K, and then increases smoothly to 0.21 at 5 K. These data suggest that the existence of strong antiferromagnetic interactions between the Mn^{III} centers of the chain resulting in a diamagnetic ground state (S = 0). This is not surprising because triply bridged Mn_2^{III} (and $Mn^{II}Mn^{III}$) dinuclear units are almost always antiferromagnetically coupled, although a dinuclear complex with the $[Mn(\mu\text{-}OMe)(\mu\text{-}O_2CR)_2Mn]$ core is not known for direct comparison. The very small increase at $T < 8$ K could be due to weak ferromagnetic interactions between the chains. This behavior is very similar to that observed for **4**, where however this behavior is more pronounced, presumably due to the stronger interactions between chains mediated by the strong hydrogen-bonding in **4**.

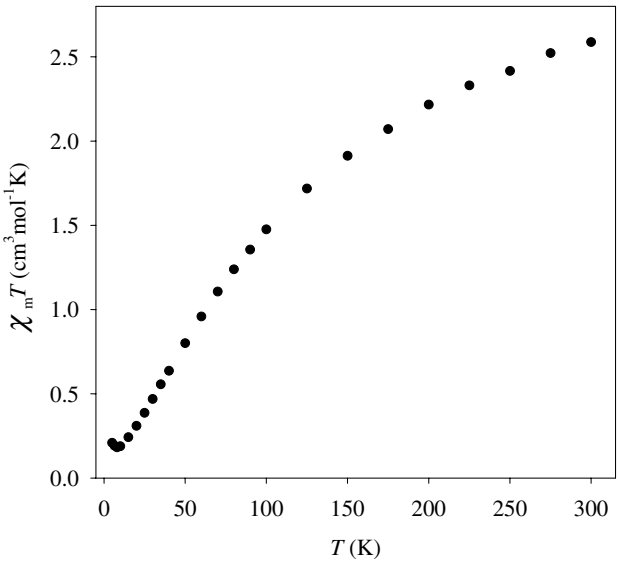

Fig. 7. A plot of $\chi_m T$ vs. T for **3**.

4. Conclusions

The new reductive aggregation procedure has led to two new compounds. The first is a variant of the $[Mn_{12}]$ family of SMMs and the second a Mn^{III} polymer. The latter is an antiferromagnetically coupled chain. In contrast, the anion of **2** is a structural variant of normal $[Mn_{12}]$ complexes, and like them is an SMM. It also displays both faster- and slower-relaxing magnetization dynamics that we assign to the presence of JT isomerism. We have in the past obtained many derivatives of $[Mn_{12}]$ complexes, for example by carboxylate substitution [6,7], one- and two-electron reduction [6f,9,10], introduction of non-carboxylate ligands [8], etc., and similar derivatization of **2** may also prove possible, in which case it is merely the prototype of what could become a large new family of related SMMs.

References

[1] (a) R. Sessoli, H.-L. Tsai, A.R. Schake, S. Wang, J.B. Vincent, K. Folting, D. Gatteschi, G. Christou, D.N. Hendrickson, J. Am. Chem. Soc. 115 (1993) 1804;
(b) R. Sessoli, D. Gatteschi, A. Caneschi, M.A. Novak, Nature 365 (1993) 141.

[2] S.M.J. Aubin, M.W. Wemple, D.M. Adams, H.-L. Tsai, G. Christou, D.N. Hendrickson, J. Am. Chem. Soc. 118 (1996) 7746.
[3] (a) G. Christou, D. Gatteschi, D.N. Hendrickson, R. Sessoli, MRS Bull. 25 (2000) 66;
(b) D. Gatteschi, R. Sessoli, Angew. Chem. Int. Ed. 42 (2003) 268.
[4] (a) A.J. Tasiopoulos, W. Wernsdorfer, B. Moulton, M.J. Zaworotko, G. Christou, J. Am. Chem. Soc. 125 (2003) 15274;
(b) A.J. Tasiopoulos, A. Vinslava, W. Wernsdorfer, K.A. Abboud, G. Christou, Angew. Chem. Int. Ed. 43 (2004) 2117;
(c) D.J. Price, S.R. Batten, B. Moubaraki, K.S. Murray, Chem. Commun. (2002) 762;
(d) S.M.J. Aubin, N.R. Dilley, L. Pardi, J. Krzystek, M.W. Wemple, L.-C. Brunel, M.B. Maple, G. Christou, D.N. Hendrickson, J. Am. Chem. Soc. 120 (1998) 4991;
(e) M. Soler, W. Wernsdorfer, K. Folting, M. Pink, G. Christou, J. Am. Chem. Soc. 126 (2004) 2156;
(f) E.K. Brechin, M. Soler, G. Christou, M. Helliwell, S.J. Teat, W. Wernsdorfer, Chem. Commun. (2003) 1276.
[5] (a) E.K. Brechin, J. Yoo, M. Nakano, J.C. Huffman, D.N. Hendrickson, G. Christou, Chem. Commun. (1999) 783;
(b) J. Yoo, E.K. Brechin, A. Yamaguchi, M. Nakano, J.C. Huffman, A.L. Maniero, L.-C. Brunel, K. Awaga, H. Ishimoto, G. Christou, D.N. Hendrickson, Inorg. Chem. 39 (2000) 3615;
(c) E.K. Brechin, M. Soler, J. Davidson, D.N. Hendrickson, S. Parsons, G. Christou, Chem. Commun. (2002) 2252;
(d) L.F. Jones, E.K. Brechin, D. Collison, A. Harrison, S.J. Teat, W. Wernsdorfer, Chem. Commun. (2002) 2974;
(e) M. Moragues-Canovas, M. Helliwell, L. Ricard, E. Riviere, W. Wersdorfer, E. Brechin, T. Mallah, Eur. J. Inorg. Chem. (2004) 2219;
(f) C.J. Milios, C.P. Raptopoulou, A. Terzis, F. Lloret, R. Vicente, S.P. Perlepes, A. Escuer, Angew. Chem. Int. Ed. 43 (2004) 210;
(g) A.K. Boudalis, B. Donnadieu, V. Nastopoulos, J.M. Clemente-Juan, A. Mari, Y. Sanakis, J.-P. Tuchagues, S.P. Perlepes, Angew. Chem. Int. Ed. 43 (2004) 2266;
(h) H. Andres, R. Basler, A.J. Blake, C. Cadiou, G. Chaboussant, C.M. Grant, H.-U. Güdel, M. Murrie, S. Parsons, C. Paulsen, F. Semadini, V. Villar, W. Wernsdorfer, R.E.P. Winpenny, Chem. Eur. J. 8 (2002) 4867.
[6] (a) S.M.J. Aubin, Z. Sun, I.A. Guzei, A.L. Rheingold, G. Christou, D.N. Hendrickson, Chem. Commun. (1997) 2239;
(b) Z. Sun, D. Ruiz, E. Rumberger, C.D. Incarvito, K. Folting, A.L. Rheingold, G. Christou, D.N. Hendrickson, Inorg. Chem. 37 (1998) 4758;
(c) D. Ruiz, Z. Sun, B. Albela, K. Folting, J. Ribas, G. Christou, D.N. Hendrickson, Angew. Chem. Int. Ed. 37 (1998) 300;
(d) Z. Sun, D. Ruiz, N.R. Dilley, M. Soler, J. Ribas, K. Folting, M.B. Maple, G. Christou, D.N. Hendrickson, Chem. Commun. (1999) 1973;
(e) S.M.J. Aubin, Z. Sun, H.J. Eppley, E.M. Rumberger, I.A. Guzei, K. Folting, P.K. Gantzel, A.L. Rheingold, G. Christou, D.N. Hendrickson, Inorg. Chem. 40 (2001) 2127;
(f) H.J. Eppley, H.-L. Tsai, N. de Vries, K. Folting, G. Christou, D.N. Hendrickson, J. Am. Chem. Soc. 117 (1995) 301;
(g) M. Soler, W. Wernsdorfer, Z. Sun, J.C. Huffman, D.N. Hendrickson, G. Christou, Chem. Commun. (2003) 2672.
[7] M. Soler, P. Artus, K. Folting, J.C. Huffman, D.N. Hendrickson, G. Christou, Inorg. Chem. 40 (2001) 4902.
[8] (a) P. Artus, C. Boskovic, J. Yoo, W.E. Streib, L.-C. Brunel, D.N. Hendrickson, G. Christou, Inorg. Chem. 40 (2001) 4199;
(b) C. Boskovic, M. Pink, J.C. Huffman, D.N. Hendrickson, G. Christou, J. Am. Chem. Soc. 123 (2001) 9914;
(c) N.E. Chakov, W. Wernsdorfer, K.A. Abboud, D.N. Hendrickson, G. Christou, Dalton Trans. (2003) 2243.
[9] (a) S.M.J. Aubin, Z. Sun, L. Pardi, J. Krzystek, K. Folting, L.-C. Brunel, A.L. Rheingold, G. Christou, D.N. Hendrickson, Inorg. Chem. 38 (1999) 5329;
(b) T. Kuroda-Sowa, M. Lam, A.L. Rheingold, C. Frommen, W.M. Reiff, M. Nakano, J. Yoo, A.L. Maniero, L.-C. Brunel, G. Christou, D.N. Hendrickson, Inorg. Chem. 40 (2001) 6469.
[10] (a) M. Soler, S.K. Chandra, D. Ruiz, E.R. Davidson, D.N. Hendrickson, G. Christou, Chem. Commun. (2000) 2417;
(b) M. Soler, W. Wernsdorfer, K.A. Abboud, J.C. Huffman, E.R. Davidson, D.N. Hendrickson, G. Christou, J. Am. Chem. Soc. 125 (2003) 3576.
[11] T. Lis, Acta Crystallogr., Sect. B 36 (1980) 2042.
[12] W. Liu, H.H. Thorp, Inorg. Chem. 32 (1993) 4102.
[13] (a) For example, see M.J. Manos, A.J. Tasiopoulos, E.J. Tolis, N. Lalioti, J.D. Woolins, A.M.Z. Slawin, M.P. Sigalas, T.A. Kabanos, Chem. Eur. J. 9 (2003) 695;
(b) H. Kang, S. Liu, S.N. Shaikh, T. Nicholson, J. Zubieta, Inorg. Chem. 28 (1989) 920.
[14] P. King, W. Wernsdorfer, K.A. Abboud, G. Christou, Inorg. Chem. 43 (2004) 7315.
[15] J.T. Brockman, J.C. Huffman, G. Christou, Angew. Chem. Int. Ed. 41 (2002) 2506.
[16] (a) A.J. Tasiopoulos, N.C. Harden, K.A. Abboud, G. Christou, Polyhedron 22 (2003) 133;
(b) D.J. Price, S.R. Batten, B. Moubaraki, K.S. Murray, Polyhedron 22 (2003) 2167.
[17] W. Wernsdorfer, E. Bonet Orozco, K. Hasselbach, A. Benoit, D. Mailly, O. Kubo, H. Nakano, B. Barbara, Phys. Rev. Lett. 79 (1997) 4014.